

Niemann–Pick C heterozygosity confers resistance to lesional necrosis and macrophage apoptosis in murine atherosclerosis

Bo Feng*[†], Dajun Zhang*[†], George Kuriakose*, Cecilia M. Devlin*, Mark Kockx[‡], and Ira Tabas*[§]

*Departments of Medicine and Anatomy and Cell Biology, Columbia University, 630 West 168th Street, New York, NY 10032; and [‡]Division of Pharmacology, University of Antwerp, Universiteitsplein 1, B-2610 Wilrijk, Belgium

Edited by Michael A. Gimbrone, Jr., Brigham and Women's Hospital, Boston, MA, and approved July 2, 2003 (received for review April 26, 2003)

Macrophage death in advanced atherosclerotic lesions leads to lesional necrosis and likely promotes plaque instability, a precursor of acute vascular events. Macrophages in advanced lesions accumulate large amounts of unesterified cholesterol, which is a potent inducer of macrophage apoptosis. We have shown recently that induction of apoptosis in cultured macrophages requires cholesterol trafficking to the endoplasmic reticulum (ER). Moreover, macrophages from mice with a heterozygous mutation in the cholesterol-trafficking protein *Npc1* have a selective defect in cholesterol trafficking to the ER and are protected from cholesterol-induced apoptosis. The goal of the present study was to test the importance of intracellular cholesterol trafficking in atherosclerotic lesional macrophage death by comparing lesion morphology in *Npc1*^{+/+};*ApoE*^{-/-} and *Npc1*^{+/-};*ApoE*^{-/-} mice. Although advanced lesions in *Npc1*^{+/+};*ApoE*^{-/-} mice had extensive acellular areas that were rich in unesterified cholesterol and macrophage debris, the lesions of *Npc1*^{+/-};*ApoE*^{-/-} mice were substantially more cellular and less necrotic. Moreover, compared with *Npc1*^{+/+};*ApoE*^{-/-} lesions, *Npc1*^{+/-};*ApoE*^{-/-} lesions had a greater number of large, TUNEL (terminal deoxynucleotidyltransferase-mediated dUTP nick end labeling)-positive areas surrounding necrotic areas, indicative of macrophage apoptosis. These differences were observed despite similar total lesion area and similar plasma lipid levels in the two groups of mice. These data provide *in vivo* evidence that intact intracellular cholesterol trafficking is important for macrophage apoptosis in advanced atherosclerotic lesions and that the ER-based model of cholesterol-induced cytotoxicity is physiologically relevant. Moreover, by showing that lesional necrosis can be diminished by a subtle defect in intracellular trafficking, these findings suggest therapeutic strategies to stabilize atherosclerotic plaques.

Macrophages are major cellular components of developing atherosclerotic lesions, and they play important roles in atherogenesis (1, 2). Interestingly, lesional macrophages undergo cell death (3, 4), although little is known about the consequences or causes of this event. Recent data with antibodies against cell-specific proteins support the idea that the macrophage is the main cell type that dies in the vicinity of lesional necrotic areas (5, 6). These necrotic areas are often found near sites of plaque rupture, which is directly linked to acute thrombosis, vascular occlusion, and tissue infarction (7). Indeed, the presence of apoptotic macrophages is associated specifically with ruptured atherosclerotic plaques in human coronary artery lesions (8). The mechanistic link between macrophage death and unstable plaques may be related to plaque-destabilizing enzymes, inflammatory mediators, and procoagulant and thrombogenic molecules released by these dying cells (2).

The causes of macrophage death in advanced atherosclerosis are not known. An important cytotoxic condition that deserves attention is excess cellular free cholesterol (FC) (9). FC accumulation in lesional foam cells has been well documented (10–14), and studies with cultured macrophages have shown that excess cellular FC is a potent inducer of cell death (15–18).

Moreover, acceleration of FC accumulation in lesional macrophages in mice by targeted disruption of *Soat1* leads to increased lesional macrophage apoptosis (19). FC-induced death in cultured macrophages, like lesional macrophage death *in vivo*, has both apoptotic and necrotic features (3, 4), and it is likely that at least a portion of the necrosis is secondary to defective phagocytic clearance of apoptotic macrophages (postapoptotic necrosis) (20, 21).

Recent work in our laboratory has revealed important mechanistic aspects of FC-induced macrophage apoptosis. By using cultured macrophages incubated with a source of lipoprotein cholesterol (acetylated low-density lipoprotein) and an acyl-CoA:cholesterol acyltransferase inhibitor to block cholesterol esterification, we have shown that apoptotic death of FC-loaded cultured macrophages is caused by both activation of Fas ligand and release of cytochrome *c* from mitochondria (17, 18). Most interestingly, FC-induced apoptosis in macrophages is entirely dependent on cholesterol trafficking to the endoplasmic reticulum (ER) (22). We have shown that FC loading of cultured macrophages activates the ER stress pathway known as the unfolded protein response (UPR) and that the branch of the UPR involving the transcription factor CHOP (C/EBP homologous protein) is necessary for execution of apoptosis in these cells (22). We have shown also that CHOP is expressed in advanced atherosclerotic lesions of *ApoE*^{-/-} mice (22).

The trafficking of lipoprotein-derived cholesterol from late endosomes to peripheral cellular membranes is dependent on the late endosomal protein *Npc1* (23–26). In the course of our mechanistic studies, we discovered that whereas complete deficiency of *Npc1* blocks cholesterol trafficking to both the plasma membrane and ER, heterozygous deficiency of *Npc1* selectively blocks cholesterol trafficking to the ER (22). Consistent with the model described above, cultured peritoneal macrophages from *Npc1*^{+/-} mice are highly resistant to FC-induced activation of the UPR and FC-induced apoptosis (22).

The goal of the present study was to determine the relevance of these concepts in advanced atherosclerotic lesions of the widely studied *ApoE*^{-/-} mouse model of atherosclerosis. We accomplished this goal by studying plaque morphology and macrophage apoptosis in advanced atherosclerotic lesions of *Npc1*^{+/+};*ApoE*^{-/-} vs. *Npc1*^{+/-};*ApoE*^{-/-} mice. Our data reveal that the *Npc1*^{+/-} mutation confers substantial resistance to lesional necrosis and lesional macrophage apoptosis. As such, these data provide *in vivo* support for the ER-based model of FC-induced apoptosis and suggest therapeutic strategies to promote plaque stability.

This paper was submitted directly (Track II) to the PNAS office.

Abbreviations: ER, endoplasmic reticulum; FC, free cholesterol; TUNEL, terminal deoxynucleotidyltransferase-mediated dUTP nick end labeling; UPR, unfolded protein response.

[†]B.F. and D.Z. contributed equally to this work.

[§]To whom correspondence should be addressed. E-mail: iat1@columbia.edu.

Materials and Methods

Mice. *Npc1*^{+/-} BALB/c mice were backcrossed into the C57BL/6 background for four generations and then bred into the *Apoe*^{-/-} C57BL/6 mouse background for an additional two generations to generate *Npc1*^{+/-};*Apoe*^{-/-} mice. These mice were bred with each other to obtain *Npc1*^{+/-};*Apoe*^{-/-} mice and *Npc1*^{+/+};*Apoe*^{-/-} mice (littermate controls) for the experiments described below. After weaning, the mice were placed on a high-cholesterol diet containing 21% anhydrous milk fat and 0.15% cholesterol ("Western-type" diet; Harlan–Teklad, Indianapolis) and killed at 18 or 25 weeks of age.

Preparation and Staining of Sections of Proximal Aortae. On the day of analysis, food was removed from the cages in the morning, and the mice were fasted for 7 h. The animals were then anesthetized, and blood was withdrawn by cardiac puncture. The heart and vascular system were perfused with PBS *in situ*, and the heart and proximal aorta were then removed surgically, embedded in OCT (optimum cutting temperature) compound (Sakura Finetek, Torrance, CA), snap frozen in an ethanol–dry-ice bath, and stored at –70°C. Sections of proximal aortae 10 μm thick were cut at –20°C by using a Microm Microtome Cryostat HM 505 E, placed on poly-L-lysine-coated slides (Fisher Scientific). The sections were then fixed in 10% buffered formalin for 5 min at room temperature and air dried for 10 min. Serial sections were stained with Harris' hematoxylin for nuclei.

Quantification of Atherosclerotic Lesion, Acellular, and Terminal Deoxynucleotidyltransferase-Mediated dUTP Nick End Labeling (TUNEL)-Positive Areas. Intimal lesional area (between the internal elastic lamina to the lumen), acellular areas (negative for hematoxylin-positive nuclei), and TUNEL-positive areas were quantified by blinded observers using a Nikon Labophot 2 microscope equipped with an Sony CCD-Iris/RGB color video camera attached to a computerized imaging system with IMAGE PRO PLUS 3.0 software. For the TUNEL technique, cryostat sections were air dried and subsequently fixed by 4% buffered formalin. We used the stringent TUNEL method described by Kockx *et al.* (27), which avoids nonspecific labeling because of active RNA synthesis.

Immunohistochemistry. The mice were anesthetized, blood was withdrawn by cardiac puncture, and the heart was perfused with PBS. The heart and proximal aorta were harvested, perfused *ex vivo* with PBS, embedded in OCT compound, and snap frozen in an ethanol–dry ice bath. For detection of the type A scavenger receptor, the frozen sections of the proximal aorta were washed in tap water and then rinsed in PBS for 5 min at room temperature. The sections were then incubated in PBS containing 2% donkey serum and 50 μg/ml rat anti-mouse macrophage type A scavenger receptor antibody (2F8; Serotec), or rat IgG2b nonimmune control antibody, for 1 h at room temperature. After washing in PBS for 5 min, the sections were incubated with the primary antibody in PBS containing 2% donkey serum. Staining was completed by incubating first with biotinylated donkey anti-rat IgG and then with streptavidin–peroxidase (Vectastain Elite ABC kit, Vector Laboratories) and 3,3'-diaminobenzidine. The sections were counterstained with hematoxylin, rinsed, mounted in Permount, and viewed with an Olympus IX 70 inverted microscope using a ×20 objective. Macrophages were detected in acetone-fixed frozen sections by using rabbit anti-mouse macrophage antiserum from Accurate Chemicals (AIA31240); rabbit nonimmune serum served as the control for this procedure.

Filipin Staining of Aortic Sections. Frozen sections of proximal aortae were washed in PBS and then fixed with fresh 3%

formaldehyde for 1 h at room temperature. The fixed sections were washed with PBS for 10 min to quench the formaldehyde and then incubated with 0.05 mg/ml filipin solution for 2 h at room temperature. After washing in PBS, the sections were viewed by fluorescence microscopy using an Olympus IX 70 inverted microscope equipped with a UV filter set (340- to 380-nm excitation, 400-nm dichroic, and 430-nm long-pass filters).

Plasma Lipid and Lipoprotein Assays. Total plasma cholesterol and phospholipids were determined by using commercial enzymatic kits (Wako, Neuss, Germany), and plasma lipoproteins were analyzed by fast performance liquid chromatography, as described (28).

Statistical Analysis. For lesional data, which are nonparametric, statistical significance was determined by the Mann–Whitney *U* test. For the quantitative TUNEL-staining data, the χ² test was used.

Results

Evidence of Necrosis, FC Accumulation, and Macrophage Debris in Advanced Atherosclerotic Lesions of *Apoe*^{-/-} Mice. *Apoe*^{-/-} mice fed a Western-type diet (high cholesterol/saturated fat) develop advanced atherosclerosis (29, 30). In preparation for experiments designed to look at the influence of the *Npc1*^{+/-} mutation on plaque morphology, we first characterized the advanced lesions of *Npc1*^{+/-};*Apoe*^{-/-} mice. As shown in Fig. 1A, raised lesions from the proximal aortae of 25-week-old *Apoe*^{-/-} mice fed a Western-type diet contained acellular regions situated beneath a layer of endothelial and intimal cells (Fig. 1, arrows). Using a stain for collagen, we focused first on acellular areas that were not simply dense fibrous scars (data not shown). Next, because extracellular FC accumulation is a property of necrotic areas of advanced atherosclerotic lesions in humans (3, 31, 32), we stained the lesions with filipin, a fluorescent dye that binds FC (31). As demonstrated in Fig. 1B, most of the acellular areas (as well as many of the cellular areas of the intima) bound filipin, whereas neither the adventitia nor the endothelium bound filipin. Moreover, the acellular areas of *Apoe*^{-/-} lesions stained only weakly with the neutral lipid dye oil red O compared with the cholesteryl ester-rich foam cell areas (data not shown); this finding indicates that the acellular areas were richer in FC than in cholesteryl esters. To determine whether these acellular areas might represent sites of macrophage death as suggested by the studies of Mitchinson and colleagues (6), we looked for the presence of macrophage proteins in the absence of intact cells (debris). As shown in Fig. 1C, many of the acellular regions reacted with an antibody against a macrophage protein, the type A scavenger receptor. In contrast, adjacent sections did not react with nonimmune control antibody (Fig. 1D). Similar results were obtained by using an antibody directed against the macrophage protein Mac-3 (data not shown). Thus, advanced lesions of *Apoe*^{-/-} mice contain acellular areas that stain for both FC and macrophage proteins, suggesting that these areas are necrotic areas containing the debris of macrophages.

Atherosclerotic Lesions of *Npc1*^{+/-};*Apoe*^{-/-} Mice Have Fewer Acellular Areas Than Lesions of *Apoe*^{-/-} Mice. To assess the effect of the heterozygous Niemann–Pick C mutation on the atherosclerotic lesion morphology, we studied 25-week-old, Western-diet-fed *Npc1*^{+/+};*Apoe*^{-/-} mice and *Npc1*^{+/-};*Apoe*^{-/-} mice. As was the case with peritoneal macrophages from these mice on the *Apoe*^{+/+} background (22), peritoneal macrophages from *Npc1*^{+/-};*Apoe*^{-/-} mice showed marked resistance to FC-induced apoptosis compared with *Npc1*^{+/+};*Apoe*^{-/-} macrophages (data not shown). Both groups of mice appeared normal, and their weights at the end of the 25-week period were not statistically

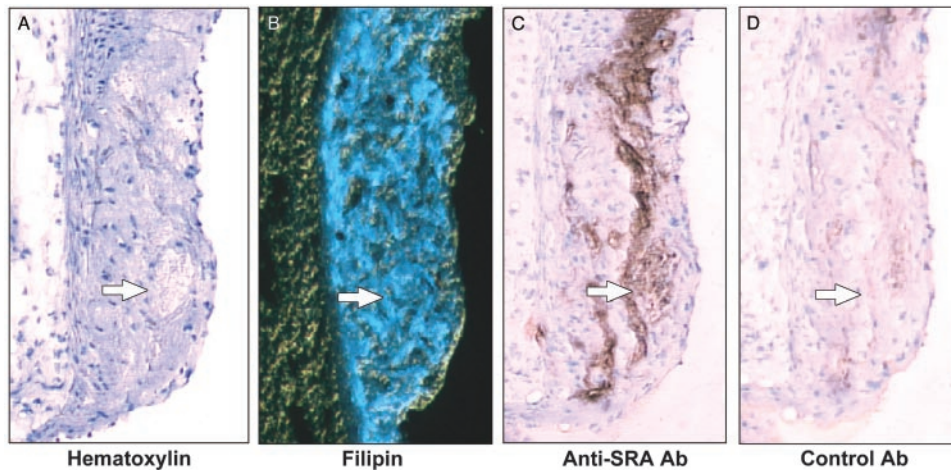


Fig. 1. Characterization of acellular areas in the advanced atherosclerotic lesions of *Apoe*^{-/-} mice. Adjacent sections of proximal aortic lesions from 25-week-old cholesterol-fed *Apoe*^{-/-} mice were stained with hematoxylin (A), filipin (B), anti-type A scavenger receptor antibody (C), or control antibody (D). Arrows indicate one of several acellular areas in each panel. (×150.)

different. The plasma cholesterol and phospholipid values were also not statistically different in the two groups of mice (Fig. 2A). Similarly, the gel-filtration profiles of the plasma lipoproteins were very similar (Fig. 2B); neither the small increase in the very low-density lipoprotein peak nor the small decrease in the low-density lipoprotein peak in the *Npc1*^{+/-};*Apoe*^{-/-} plasma shown in this figure was a consistent finding in repeat experiments.

An example of a histological section from each type of mouse is shown in Fig. 3. Fig. 3A shows extensive acellular areas (asterisks) in the lesion of an *Npc1*^{+/+};*Apoe*^{-/-} mouse. In contrast, the atherosclerotic lesions of the *Npc1*^{+/-};*Apoe*^{-/-} mice contained many more live cells (Fig. 3B), which were identified as macrophages by reactivity with a rabbit anti-mouse macrophage antiserum (Fig. 3C). The acellular areas in Fig. 3A

occupy a substantial amount of lesional volume, which can account for the similar overall sizes of the *Npc1*^{+/+} and *Npc1*^{+/-} lesions despite their difference in cellularity. The increased cellularity in the *Npc1*^{+/-} could be due to less accumulation of total lesional FC rather than altered intracellular location of this FC, as our model suggests. To assess this possibility, lesions from *Npc1*^{+/+};*Apoe*^{-/-} and *Npc1*^{+/-};*Apoe*^{-/-} mice were stained with filipin. As shown in Fig. 3D and E, the intensity of filipin staining was similar in the two lesions, suggesting that the increase in cellularity in the *Npc1*^{+/-};*Apoe*^{-/-} mice was not simply due to a marked decrease in overall lesional FC accumulation.

Quantitative data for two separate experiments completed ≈1 year apart are shown in Fig. 4. In the first experiment, total lesion area in the proximal aortae of *Npc1*^{+/-};*Apoe*^{-/-} mice was decreased ≈20% compared with *Npc1*^{+/+};*Apoe*^{-/-} mice (Fig.

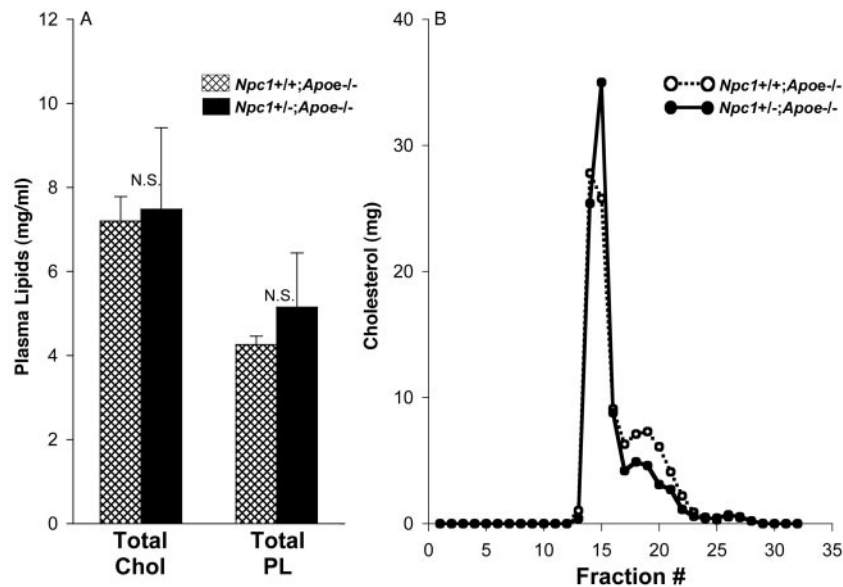


Fig. 2. Plasma lipids and lipoprotein profile of *Npc1*^{+/+};*Apoe*^{-/-} and *Npc1*^{+/-};*Apoe*^{-/-} mice. (A) Plasma samples of 25-week-old cholesterol-fed *Npc1*^{+/+};*Apoe*^{-/-} mice (14 females and 12 males, cross-hatched bars) and *Npc1*^{+/-};*Apoe*^{-/-} mice (3 females and 6 males, solid bars) were assayed for cholesterol (Chol) and phospholipid (PL) concentrations. The differences in both cholesterol and phospholipid levels between the two groups of mice were not statistically significant. (B) Pooled plasma samples from two male *Npc1*^{+/+};*Apoe*^{-/-} (○) and two male *Npc1*^{+/-};*Apoe*^{-/-} (●) mice were subjected to fast performance liquid chromatography gel-filtration fractionation. The small difference between the two groups of mice in the fast performance liquid chromatography peak around fraction 18 was not observed in repeat experiments.

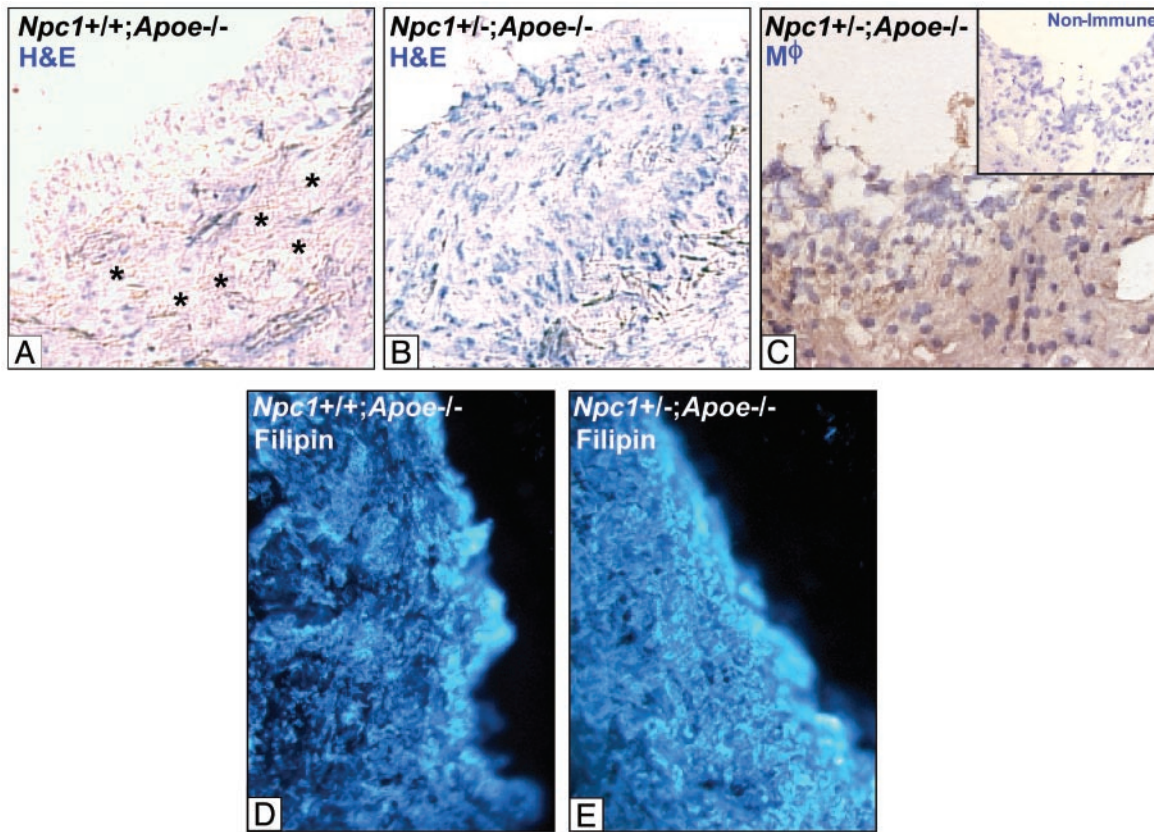


Fig. 3. Hematoxylin, macrophage, and filipin staining of proximal aortic lesion sections from male *Npc1*^{+/+};*ApoE*^{-/-} and *Npc1*^{+/-};*ApoE*^{-/-} mice. (A and B) Sections of proximal aortic lesions from 25-week-old cholesterol-fed male *Npc1*^{+/+};*ApoE*^{-/-} (A) and *Npc1*^{+/-};*ApoE*^{-/-} mice (B). Sections were stained with hematoxylin and eosin (H&E). (×225.) Asterisks indicate acellular areas. The lesion from the *Npc1*^{+/+};*ApoE*^{-/-} mouse (B) is markedly more cellular than the lesion from the *Npc1*^{+/+};*ApoE*^{-/-} mouse (A). (C) These cells were identified as macrophages (Mφ) by immunohistochemistry. *Inset* shows a nonimmune control. (D and E) Lesions from these mice were stained with filipin. Overall lesional accumulation of FC was not markedly different in the two lesions.

4A), but this difference was not statistically significant. The acellular areas of the *Npc1*^{+/-};*ApoE*^{-/-} lesions, however, were decreased by ≈50% (Fig. 4B). Therefore, when the data were expressed as percent acellular area, there was a substantial and highly statistically significant difference between the two groups of mice (Fig. 4C). The decrease in acellular areas in the lesions of *Npc1*^{+/-};*ApoE*^{-/-} mice was similar in males and females (data not shown). In the repeat experiment, lesion area *per se* was almost identical between the two groups of mice (Fig. 4D), and acellular areas were decreased by ≈35% (Fig. 4E and F), which reached a very high level of statistical difference. Thus, the proximal aortic lesions of 25-week-old *Npc1*^{+/-};*ApoE*^{-/-} mice have less extensive acellular areas than those of *Npc1*^{+/+};*ApoE*^{-/-} mice.

Atherosclerotic Lesions of *Npc1*^{+/-};*ApoE*^{-/-} Mice Have Fewer TUNEL-Positive Apoptotic Areas Than Lesions of *Npc1*^{+/+};*ApoE*^{-/-} Mice. To assess apoptosis in these lesions, sections were stained by using a stringent modification of the TUNEL method (27). Examples of sections from two *Npc1*^{+/+};*ApoE*^{-/-} mice are shown in Fig. 5A and A'. In both of these examples, large TUNEL-positive areas were present; in Fig. 5A such an area was located near an area of widespread necrosis. In the sections from two *Npc1*^{+/-};*ApoE*^{-/-} mice (Fig. 5B and B'), TUNEL staining either was not seen or was less extensive. Fig. 5C and D show the quantification of lesion area and TUNEL data, respectively, for nine *Npc1*^{+/+};*ApoE*^{-/-} mice and seven *Npc1*^{+/-};*ApoE*^{-/-} mice. Fewer of the *Npc1*^{+/-};*ApoE*^{-/-} lesions contained apoptotic, TUNEL-positive areas despite no significant

change in lesion size. Thus, lesional macrophage death is decreased by a mutation that confers a specific defect in intracellular cholesterol trafficking to the ER.

Discussion

Few studies have attempted to link genetic alterations in specific macrophage death pathways directly with consequences for atherosclerotic lesion morphology *in vivo*. In the current study, this strategy was inspired by two recent findings by our laboratory using cultured peritoneal macrophages: (i) cholesterol trafficking to the ER, by activation of the ER-based UPR, is necessary for FC-induced apoptosis in macrophages (22), and (ii) macrophages with the *Npc1*^{+/-} mutation have a specific defect in the trafficking of lipoprotein-derived cholesterol to the ER, resulting in abrogation of both FC-induced UPR activation and FC-induced apoptosis (22). Moreover, the UPR-induced transcription factor CHOP (C/EBP homologous protein) is expressed in atherosclerotic lesions of *ApoE*^{-/-} mice (22). These previous data were conducted with cells in culture, and the physiological relevance of the method used for FC loading (acylated low-density lipoprotein plus an acyl-CoA:cholesterol acyltransferase inhibitor) was uncertain. Thus, it was critical to seek evidence for or against the FC-ER-based model of macrophage death in lesional macrophage apoptosis *in vivo*. The finding that lesional necrosis and macrophage apoptosis were substantially less in the lesions of a mouse with a subtle defect in cholesterol trafficking to the ER provides strong support for this model.

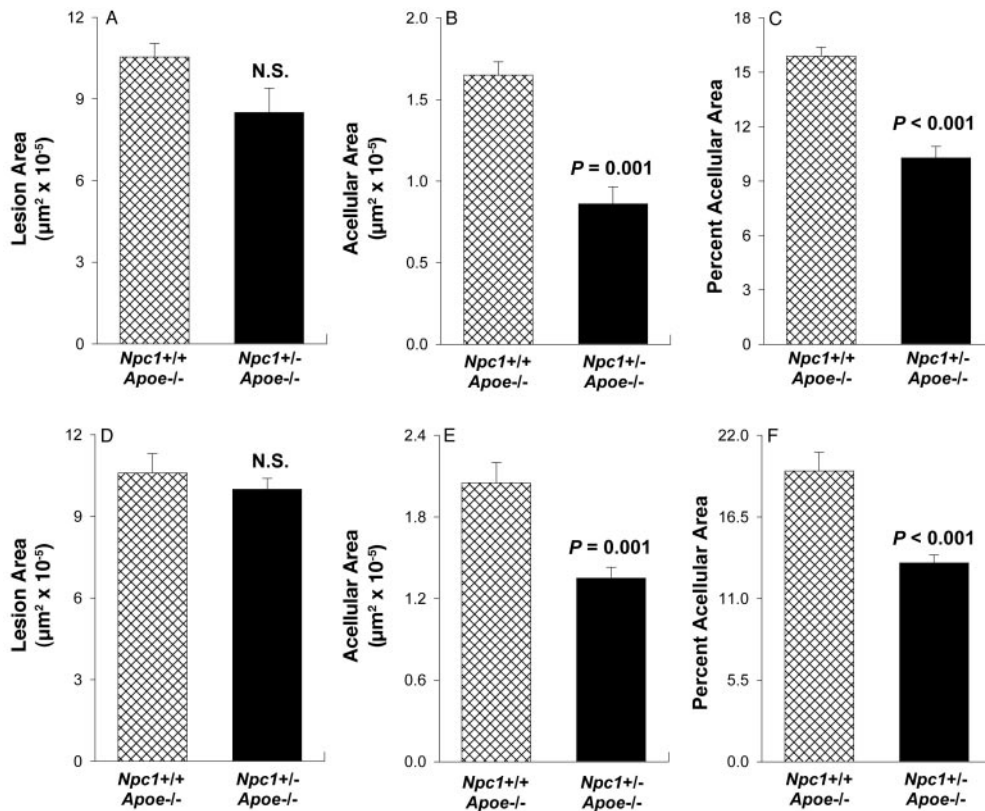


Fig. 4. Quantification of atherosclerotic lesion area and acellular area in the proximal aortae of *Npc1*^{+/+}*Apoe*^{-/-} and *Npc1*^{+/-}*Apoe*^{-/-} mice. Analyses were conducted ≈1 year apart on two separate groups of mice. In experiment 1 (A–C), the proximal aortae from 25-week-old cholesterol-fed *Npc1*^{+/+}*Apoe*^{-/-} mice (14 females and 12 males, cross-hatched bars) and *Npc1*^{+/-}*Apoe*^{-/-} mice (3 females and 6 males, solid bars) were assayed for average atherosclerotic lesion area (A) and acellular area (B). (C) The data are expressed as percent acellular area [(acellular area/lesion area) × 100]. In experiment 2 (D–F), the same analyses are displayed in D, E, and F, respectively. There were 13 *Npc1*^{+/+}*Apoe*^{-/-} mice (5 females and 8 males) and 15 *Npc1*^{+/-}*Apoe*^{-/-} mice (9 females and 6 males). Using the Mann–Whitney *U* test, we found that the difference in lesion area between the two groups of mice in both experiments was not statistically significant, whereas the difference was highly statistically significant for acellular area ($P = 0.001$) and percent acellular area ($P < 0.001$) in both experiments.

What is the physiological significance of increased macrophage cellularity and decreased apoptosis in *Npc1*^{+/-}*Apoe*^{-/-} lesions? Although it is theoretically possible that increased numbers of macrophages could contribute to lesion pathology

(33), overall lesion size was not increased in the *Npc1*^{+/-}*Apoe*^{-/-} mouse model. Rather, the increased cellularity was associated with less lesional necrosis. There is evidence that macrophage death contributes to the development of lesional

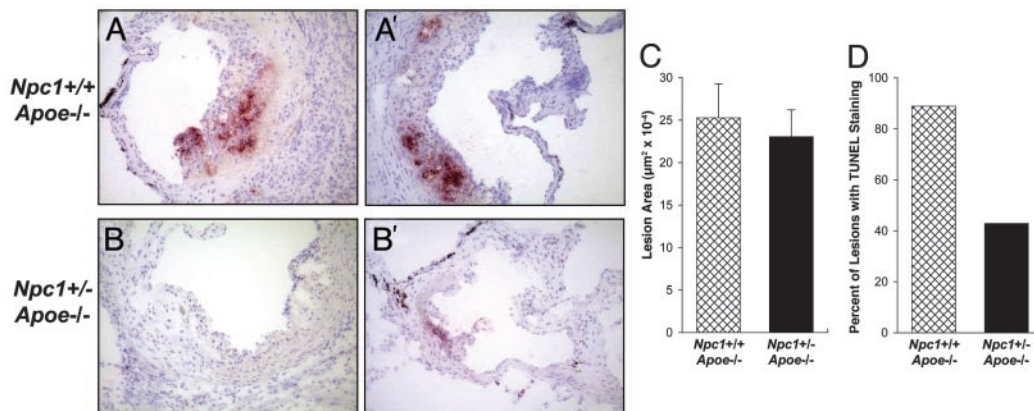


Fig. 5. TUNEL staining of lesions in the proximal aortae of *Npc1*^{+/+}*Apoe*^{-/-} and *Npc1*^{+/-}*Apoe*^{-/-} mice. Atherosclerotic lesions in the proximal aortae of nine 18-week-old cholesterol-fed *Npc1*^{+/+}*Apoe*^{-/-} mice and seven *Npc1*^{+/-}*Apoe*^{-/-} mice were assayed for TUNEL positivity. Examples of representative sections from two *Npc1*^{+/+}*Apoe*^{-/-} mice (A and A') and two *Npc1*^{+/-}*Apoe*^{-/-} mice (B and B') are shown. (×20.) Quantification of total lesion area and the percentage of mice that had TUNEL-positive lesions are shown in C and D, respectively. For the TUNEL analysis, two aortic sections were examined per mouse. Using the Mann–Whitney *U* test, we found that the difference in lesion area between the two groups of mice was not statistically significant, whereas the difference in TUNEL positivity was found to be statistically significant by the χ^2 test ($P < 0.05$).

necrotic areas, which have been called “a graveyard of dead macrophages” (34). For example, necrotic areas of human lesions have been shown to contain macrophage proteins (5, 6), consistent with our data (Fig. 1C), and dying macrophages are often found in the vicinity of lesional necrosis (2, 3, 32). Because atherosclerotic lesions rich in necrotic areas are susceptible to plaque rupture, acute thrombosis, and acute vascular occlusion (7), the increase in cellularity may be a sign of plaque stabilization. Future studies will be needed to determine whether *Npc1*^{+/-}; *ApoE*^{-/-} lesions are indeed less susceptible to plaque rupture *per se*.

In summary, we have demonstrated that partial dysfunction of a specific protein involved in cholesterol trafficking is associated with increased cellularity and less apoptosis in advanced atherosclerotic lesions. These findings highlight important issues

related to mechanisms, consequences, and potential therapeutic implications of FC-induced macrophage death during the progression of atherosclerosis. Regarding the potential for therapy, we have shown that very low doses of cholesterol-trafficking inhibitor U18666A selectively inhibit cholesterol trafficking to the ER and block UPR activation and apoptosis in FC-loaded cultured macrophages almost completely (22). Furthermore, the atherosclerosis data raise the interesting question whether heterozygous Niemann–Pick C humans, who are reported to be “normal” (35), actually have a lower incidence of acute ischemic events compared with individuals without this mutation.

We thank Dr. Peter Pentchev for providing the *Npc1*^{-/-} mice. This work was supported by National Institutes of Health Grants HL54591 and HL56984 (to I.T.).

1. Ross, R. (1995) *Annu. Rev. Physiol.* **57**, 791–804.
2. Libby, P. & Clinton, S. K. (1993) *Curr. Opin. Lipidol.* **4**, 355–363.
3. Mitchinson, M. J., Hardwick, S. J. & Bennett, M. R. (1996) *Curr. Opin. Lipidol.* **7**, 324–329.
4. Kockx, M. M. (1998) *Arterioscler. Thromb. Vasc. Biol.* **18**, 1519–1522.
5. Berberian, P. A., Myers, W., Tytell, M., Challa, V. & Bond, M. G. (1990) *Am. J. Pathol.* **136**, 71–80.
6. Ball, R. Y., Stowers, E. C., Burton, J. H., Cary, N. R., Skepper, J. N. & Mitchinson, M. J. (1995) *Atherosclerosis (Shannon, Irel.)* **114**, 45–54.
7. Fuster, V., Badimon, L., Badimon, J. J. & Chesebro, J. H. (1992) *N. Engl. J. Med.* **326**, 242–250.
8. Kolodgie, F. D., Narula, J., Burke, A. P., Haider, N., Farb, A., Hui-Liang, Y., Smialek, J. & Virmani, R. (2000) *Am. J. Pathol.* **157**, 1259–1268.
9. Tabas, I. (1997) *Trends Cardiovasc. Med.* **7**, 256–263.
10. Shio, H., Haley, N. J. & Fowler, S. (1979) *Lab. Invest.* **41**, 160–167.
11. Rapp, J. H., Connor, W. E., Lin, D. S., Inahara, T. & Porter, J. M. (1983) *J. Lipid Res.* **24**, 1329–1335.
12. Small, D. M., Bond, M. G., Waugh, D., Prack, M. & Sawyer, J. K. (1984) *J. Clin. Invest.* **73**, 1590–1605.
13. Kruth, H. S. & Fry, D. L. (1984) *Exp. Mol. Pathol.* **40**, 288–294.
14. Lundberg, B. (1985) *Atherosclerosis (Shannon, Irel.)* **56**, 93–110.
15. Warner, G. J., Stoudt, G., Bamberger, M., Johnson, W. J. & Rothblat, G. H. (1995) *J. Biol. Chem.* **270**, 5772–5778.
16. Tabas, I., Marathe, S., Keesler, G. A., Beatini, N. & Shiratori, Y. (1996) *J. Biol. Chem.* **271**, 22773–22781.
17. Yao, P. M. & Tabas, I. (2000) *J. Biol. Chem.* **275**, 23807–23813.
18. Yao, P. M. & Tabas, I. (2001) *J. Biol. Chem.* **276**, 42468–42476.
19. Fazio, S., Major, A. S., Swift, L. L., Gleaves, L. A., Accad, M., Linton, M. F. & Farese, R. V., Jr. (2001) *J. Clin. Invest.* **107**, 163–171.
20. Chang, M.-K., Bergmark, C., Laurila, A., Horkko, S., Han, K.-H., Friedman, P., Dennis, E. A. & Witztum, J. L. (1999) *Proc. Natl. Acad. Sci. USA* **96**, 6353–6358.
21. Lemasters, J. J. (1999) *Am. J. Physiol.* **276**, G1–G6.
22. Feng, B., Yao, P. M., Li, Y., Devlin, C. M., Zhang, D., Harding, H. P., Sweeney, M., Rong, J. X., Kuriakose, G., Fisher, E. A., et al. (2003) *Nat. Cell Biol.*, in press.
23. Pentchev, P. G., Boothe, A. D., Kruth, H. S., Weintraub, H., Stivers, J. & Brady, R. O. (1984) *J. Biol. Chem.* **259**, 5784–5791.
24. Loftus, S. K., Morris, J. A., Carstea, E. D., Gu, J. Z., Cummings, C., Brown, A., Ellison, J., Ohno, K., Rosenfeld, M. A., Tagle, D. A., et al. (1997) *Science* **277**, 232–235.
25. Liscum, L. & Klansek, J. J. (1998) *Curr. Opin. Lipidol.* **9**, 131–135.
26. Pentchev, P. G., Blanchette-Mackie, E. J. & Liscum, L. (1997) *Subcell. Biochem.* **28**, 437–451.
27. Kockx, M. M., Muhring, J., Knaepen, M. W. & De Meyer, G. R. (1998) *Am. J. Pathol.* **152**, 885–888.
28. Devlin, C. M., Kuriakose, G., Hirsch, E. & Tabas, I. (2002) *Proc. Natl. Acad. Sci. USA* **99**, 6280–6285.
29. Nakashima, Y., Plump, A. S., Raines, E. W., Breslow, J. L. & Ross, R. (1994) *Arterioscler. Thromb.* **14**, 133–140.
30. Reddick, R. L., Zhang, S. H. & Maeda, N. (1994) *Arterioscler. Thromb.* **14**, 141–147.
31. Kruth, H. S. (1985) *Atherosclerosis (Shannon, Irel.)* **57**, 337–341.
32. Guyton, J. R. & Klemp, K. F. (1996) *Arterioscler. Thromb. Vasc. Biol.* **16**, 4–11.
33. Smith, J. D., Trogan, E., Ginsberg, M., Grigaux, C., Tian, J. & Miyata, M. (1995) *Proc. Natl. Acad. Sci. USA* **92**, 8264–8268.
34. Schaefer, H. E. (1981) in *Disorders of the Monocyte-Macrophage System*, eds. Schmalze, F., Huhn, D. & Schaefer, H. E. (Springer, Berlin), pp. 137–142.
35. Pentchev, P. G., Vanier, M. T., Suzuki, K. & Patterson, M. C. (1995) in *Metabolic Basis of Inherited Disease*, eds. Scriver, C. R., Beaudet, A. L., Sly, W. S. & Valle, D. (McGraw–Hill, New York), pp. 2625–2639.